Published in final edited form as:
Cytotherapy. 2013 May ; 15(5): 586–597. doi:10.1016/j.jcyt.2013.01.006.

Naïve rat umbilical cord matrix stem cells significantly attenuate mammary tumor growth through modulation of endogenous immune responses

Atsushi Kawabata[1], **Naomi Ohta**[1], **Garret Seiler**[1], **Marla M. Pyle**[1], **Susumu Ishiguro**[1], **Yong Qing Zhang**[2], **Kevin G. Becker**[2], **Deryl Troyer**[1], and **Masaaki Tamura**[1]

[1]Department of Anatomy & Physiology, Kansas State University, College of Veterinary Medicine, Manhattan, Kansas

[2]Gene Expression and Genomics Unit, NIH Biomedical Research Center, National Institute on Aging, NIH, Baltimore, Maryland, USA

Abstract

Background aims—Un-engineered human and rat umbilical cord matrix stem cells (UCMSCs) attenuate growth of several types of tumors in mice and rats. However, the mechanism by which UCMSCs attenuate tumor growth has not been studied rigorously.

Methods—The possible mechanisms of tumor growth attenuation by rat UCMSCs were studied using orthotopic Mat B III rat mammary tumor grafts in female F344 rats. Tumor-infiltrating leukocytes were identified and quantified by immunohistochemistry analysis. Potential cytokines involved in lymphocyte infiltration in the tumors were determined by microarray and Western blot analysis. The Boyden chamber migration assay was performed for the functional analysis of identified cytokines.

Results—Rat UCMSCs markedly attenuated tumor growth; this attenuation was accompanied by considerable lymphocyte infiltration. Immunohistochemistry analysis revealed that most infiltrating lymphocytes in the rat UCMSC-treated tumors were $CD3^+$ T cells. In addition, treatment with rat UCMSCs significantly increased infiltration of $CD8^+$ and $CD4^+$ T cells and natural killer (NK) cells throughout tumor tissue. $CD68^+$ monocytes/macrophages and $Foxp3^+$ regulatory T cells were scarcely observed, only in the tumors of the phosphate-buffered saline control group. Microarray analysis of rat UCMSCs demonstrated that monocyte chemotactic protein-1 is involved in rat UCMSC-induced lymphocyte infiltration in the tumor tissues.

Conclusions—These results suggest that naïve rat UCMSCs attenuated mammary tumor growth at least in part by enhancing host anti-tumor immune responses. Naïve UCMSCs can be used as powerful therapeutic cells for breast cancer treatment, and monocyte chemotactic protein-1 may be a key molecule to enhance the effect of UCMSCs at the tumor site.

Keywords

immune response; macrophages; mammary tumor; rat umbilical cord matrix stem cells; T cells

Correspondence: Dr Masaaki Tamura, Department of Anatomy & Physiology, Kansas State University, College of Veterinary Medicine, Manhattan, KS 66506. mtamura@vet.ksu.edu.

Disclosure of interest: The authors have no commercial, proprietary, or financial interest in the products or companies described in this article.

Introduction

We have isolated a cell line from Wharton's jelly of rat umbilical cord, termed rat umbilical cord matrix stem cells (UCMSCs) (1). Characteristics of these rat UCMSCs are similar to cells isolated from human umbilical cord matrix and bone marrow (2,3). Both human and rat UCMSCs exhibit tumor tropism (1,4–6). Human UCMSCs have proven to be useful as gene delivery vehicles for targeted gene therapy (4,6). We previously discovered that intratumoral or intravenous injection of naïve rat UCMSCs is capable of causing complete regression of rat mammary tumors in immunocompetent rats (1). More recent studies also indicated that naïve human UCMSCs alone possess strong tumoricidal activity against human breast carcinoma cells in immunodeficient mice (5,7). Both human and rat UCMSCs have been shown to induce apoptosis and cell cycle arrest in co-cultured tumor cells by UCMSC-produced tumor cell growth regulators (1,5,7). Genome-wide microarray analysis revealed that these growth regulators are potentially associated with multiple tumor suppressor gene products (8) and cell motilityassociated genes (7). These results suggest that naïve UCMSCs can be used for cytotherapy for mammary tumors. However, the mechanism by which UCMSCs control tumor growth in immunocompetent animals is not yet completely understood.

The tumor micro-environment, composed of various cell types such as endothelial cells, tumor-infiltrating leukocytes (TILs), fibroblasts and extracellular matrix, is important in regulating tumor growth (9–13). Fleming *et al.* (13) showed that breast extracellular matrix has an ability to increase the aggressiveness and tumorigenicity of breast cancer cells. However, a suppressive role for stromal cells in the tumor micro-environment is also reported (14−17). Among components in the tumor microenvironment, TILs play an important role in tumor attenuation (18,19). In particular, two subsets of lymphocytes, $CD8^+$ T cells and NK cells, are suggested to be involved in tumor attenuation by directly damaging tumor cells (19,20). This suggestion is supported by reports that TILs can provide a survival advantage to various cancer patients (20−24). In contrast, regulatory T (Treg) cells, a sub-population of T cells that have the ability to suppress both $CD4^+$ and $CD8^+$ T-cell functions (25), indirectly support tumor growth by suppressing tumor-specific $CD8^+$ T cells (26).

Although both naïve human and rat UCMSCs exhibited strong tumoricidal activity against breast carcinoma cells, a bolus treatment with rat UCMSCs caused complete tumor regression in immunocompetent rats (1), whereas human UCMSCs did not show such powerful tumor growth attenuation effects in an animal study in immunodeficient mice; treatment with human UCMSCs reduced tumor burden by 50% (5). These studies prompted us to speculate an involvement of tumor immune response in rat UCMSCdependent strong tumoricidal activity because only immunocompetent animals were used for the rat UCMSC study. In support of this speculation, lymphocyte infiltration in tumor tissues has been shown to be well correlated with good clinical outcomes in human patients receiving tumor antigen-activated $CD8^+$ T-cell infusions for metastatic melanoma (27).

In the present study, we attempted to clarify the mechanisms by which naïve rat UCMSCs cause attenuation or regression of tumor growth *in vivo* and *in vitro*. We report here for the first time that treatment with rat UCMSCs significantly increases lymphocyte infiltration in the tumor tissues and that TILs, primarily $CD8^+$ T cells and NK cells, induce tumor cell death, causing regression of tumors. The primary mechanism by which rat UCMSCs caused significant lymphocyte infiltration in the tumor tissues appears to be due to the increased monocyte chemotactic protein-1 (MCP-1) secretion from rat UCMSCs that had homed tumor tissues.

Methods

Cell culture

Rat UCMSCs were harvested from E19 pregnant rats. The method to isolate and culture rat UCMSCs was previously described (1). Rat UCMSCs were maintained in low-serum (defined) medium, containing the following mixture per 100 mL: 57 mL low-glucose Dulbecco's modified Eagle medium (Invitrogen, Carlsbad, CA, USA), 37 mL MCBD 201 Medium (Sigma-Aldrich, St Louis, MO, USA), 2 mL fetal bovine serum (Atlanta Biologicals, Inc, Lawrenceville, GA, USA), 1 mL of 100× Insulin-Transferrin-Selenium-X (Invitrogen), 1 mL of 0.15 g/mL AlbuMAX I (Invitrogen), 1 mL of 100× Pen-Strep (Invitrogen), 10 nmol/L dexamethasone (Sigma), 100 μmol/L ascorbic acid 2-phosphate (Sigma), 10 ng/mL epidermal growth factor (R&D Systems, Minneapolis, MN, USA) and 10 ng/mL platelet-derived growth factor-BB (R&D Systems). Cells were maintained at 37°C in a humidified atmosphere containing 5% carbon dioxide. The rat mammary adenocarcinoma cell line, Mat B III (American Type Culture Collection, Manassas, VA, USA), was maintained in McCoy's 5A modified medium (Invitrogen) supplemented with 10% fetal bovine serum, 100 units/mL penicillin, and 100 μg/mL streptomycin (Invitrogen). Cells were cultured at 37°C in a humidified atmosphere containing 5% carbon dioxide.

In vivo studies

All experiments were performed using protocols approved by the Institutional Animal Care and Use Committee of Kansas State University (#2681). Female 4- to 5-month-old F344 rats were obtained from Charles River Laboratories (Wilmington, MA, USA). All rats were housed in a clean facility and held for 1 week to acclimatize. On day 0, 1×10^5 Mat B III cells suspended in 100 μL of phosphatebuffered saline (PBS) were implanted orthotopically into the abdominal mammary fat pad under isoflurane anesthesia. All rats were randomly assigned to two treatment groups: intratumoral PBS injection (n = 5) and intratumoral rat UCMSC (1×10^6) transplant (n = 9). On day 4 after tumor cell transplantation, rat UCMSCs (1×10^6) suspended in 100 μL of PBS were administered via intratumoral injection. Tumor-bearing rats given 100 μL of PBS via intratumoral injection on day 4 served as control rats. Tumors became palpable starting from day 7; tumors were measured every 3–4 days with calipers under isoflurane anesthesia. Some rat UCMSC-treated rats (five rats) and PBS-treated rats were sacrificed 14 days after tumor cell inoculation. Tumor tissues were removed, fixed in 10% buffered neutral formalin and used for histologic and immunohistochemistry analysis. Fresh-frozen tissue was also prepared using O.C.T. Compound (Sakura Finetek USA, Inc, Torrance, CA, USA). The remaining four rat UCMSC-treated rats were used for monitoring of the tumor size until the tumor size was insignificant.

Microarray analysis

To examine chemoattractant gene expression, a microarray study was performed comparing naïve rat UCMSCs and rat UCMSCs co-cultured with Mat B III cells. Rat UCMSCs and Mat B III cells were co-cultured using 10-cm Transwell culture dishes in which the insert membrane pore size is 0.4 μm (Corning Life Sciences, Lowell, MA, USA). Rat UCMSCs (1×10^5) were seeded in the bottom culture plate, and Mat B III cells (1.5×10^6) were added to the insert on the following day. After co-culture for 48 h, total RNAs were isolated using TRIzol Reagent (Invitrogen) following the manufacturer's instructions. Quality and quantity of total RNA samples were assessed using an Agilent 2100 Bioanalyzer (Agilent Technologies, Palo Alto, CA, USA). The microarray analysis, including quality control, was conducted by the Gene Expression and Genomics Unit at the National Institute on Aging (NIA) using RatRef-12 Expression BeadChip (Illumina, San Diego, CA, USA). For each sample, biotinylated complementary RNA was prepared using an Illumina TotalPrep RNA

Amplification Kit (Applied Biosystems, Foster City, CA, USA). Overall microarray analysis was performed according to the method described previously (28). Statistical analysis was processed using a *z* score developed at NIA (29). The *z* scores were calculated by subtracting the average gene intensity from the raw intensity data for each gene and dividing that result by the standard deviation of all the measured intensities. Gene expression differences between any two experiments were calculated by taking the difference between the observed gene *z* scores. Genes relevant to cell migration, such as chemokines and cytokines, which showed 1.5 times higher expression than in the control group, were selected for the final gene list.

Cell migration assay

Migration assay of peripheral blood mononuclear cells (PBMCs) was carried out using Transwell cell culture plates with 5-μm pores (Corning Life Sciences) according to the previously described method (30). The bottom membrane of the Transwell inserts was coated with Matrigel (200 μg/mL; BD Biosciences, Rockville, MD, USA) before use. In the bottom of the Transwell culture plate, 3×10^4 rat UCMSCs or Mat B III cells were seeded and cultured for 24 h. PBMCs (0.5×10^5) isolated from the peripheral blood obtained from an adult female F344 rat were suspended in 100 μL of defined medium and added to the Transwell insert. Antibodies against MCP-1 (Santa Cruz Biotechnology, Santa Cruz, CA, USA) or control IgG were added in the lower chamber at a concentration of 2 μg/well or 4 μg/well 3 h before the addition of PBMCs. Cells were incubated at 37°C for 3 h. At the end of the incubation, the membrane of the Transwell insert was fixed in methanol, stained with Giemsa solution for 15 min and dried overnight. The membrane was removed from the insert and embedded in Permount Mounting Medium (Fisher Scientific, Pittsburgh, PA, USA). The number of PBMCs stained with Giemsa solution on the underside of the membrane (i.e., the side facing the rat UCMSCs or Mat B III cells in the bottom chamber) was counted under the microscope.

Comparison of expression of MCP-1 in rat UCMSCs and Mat B III by Western blot analysis

Western blot analysis was performed to examine chemoattractant protein expression. Rat UCMSCs and Mat B III cells were co-cultured using six-well Transwell culture plates in which the insert membrane pore size is 0.4 μm (Corning Life Sciences). Rat UCMSCs (5×10^3) were seeded in the bottom culture plate, and Mat B III cells (7.5×10^4) were added to the insert on the following day. After co-culture for 72 h, total cellular protein of rat UCMSCs or Mat B III cells was prepared using RIPA Buffer (Sigma). Protein samples were separated by 12% SDS-PAGE, electroblotted onto nitrocellulose membrane (GE Healthcare, Uppsala, Sweden) and blocked with 4% non-fat dry milk in 0.1% Tween 20 (Fisher Scientific) in PBS for 1 h at room temperature. The membranes were washed and incubated with antibody against MCP-1 (1:200; Santa Cruz Biotechnology) with 4% non-fat dry milk in 0.1% Tween 20 in PBS for 1 h at room temperature, followed by incubation with a horseradish peroxidase-conjugated anti-rabbit IgG secondary antibody (1:2000; GE Healthcare) for 1 h at room temperature. The protein expression signal was detected with SuperSignal West Femto Maximum Sensitivity Substrate (Pierce, Rockford, IL, USA). Glyceraldehyde-3-phosphate dehydrogenase (GAPDH) was used as the loading control of sample by re-probing with an anti-GAPDH antibody (1:2000; Santa Cruz Biotechnology).

Histologic analysis

Paraffin-embedded mammary tumor tissues were sectioned at 4 μm and stained with hematoxylin and eosin for histologic examination. Some unstained sections were selected for immunohistochemistry to determine the CD antigens on the lymphocytes in the tumor tissues. Slides were de-paraffinized and rehydrated before staining. The heat-induced antigen un-masking was performed in citrate buffer for 5 min using an autoclave. Sections

were incubated with 3% hydrogen peroxide in methanol for 3 min to block endogenous peroxide activity. For CD4 and Foxp3 immunostaining, fresh-frozen tissue sections (4 μm) fixed by acetone were prepared and incubated in 4% non-fat skim milk in PBS at room temperature for 20 min. The dilution of antibodies for CD3 (Dako North America, Carpinteria, CA, USA), CD8 (BD Biosciences), CD20 (Santa Cruz Biotechnology) and CD68 (Santa Cruz Biotechnology) was 1:50. The dilution of antibodies for CD4 (AbD Serotec, Raleigh, NC, USA), Foxp3 (Aviva Systems Biology, San Diego, CA, USA) and NK cell marker (Santa Cruz Biotechnology) was 1:100. Sections were incubated with the primary antibodies for 60 min at room temperature. For immunostaining for CD4 and CD20, sections were incubated with biotinconjugated antibody against mouse IgG and goat IgG (Vector Laboratories, Burlingame, CA, USA) followed by reaction with the avidin-biotin peroxidase complex reagent (Vector Laboratories) for 40 min at room temperature. For immunostaining for CD3, CD8 and CD68, Foxp3 and NK cell marker, sections were incubated with biotin-conjugated antibody against rabbit IgG (Vector Laboratories) before reaction with the avidin-biotin peroxidase complex reagent (Vector Laboratories). Peroxidase activity was visualized with 3,3′-diaminobenzidine tetrahydrochloride (Sigma). Sections were lightly counterstained with Mayer's hematoxylin. The average number of each cell type (bar graphs) was determined by analyzing 10 tumor areas in each treatment group and was expressed as cell number per high-power field (400×).

Statistical analysis

All data are reported as mean ± SE. Data were analyzed by Student *t* test. Group comparisons were deemed significant for two-tailed *P* values < 0.05.

Results

Rat UCMSC treatment significantly attenuated growth of mammary tumor grafts in vivo

Intratumoral injection of rat UCMSCs significantly attenuated the growth of orthotopic grafts of rat mammary tumors compared with PBS-injected control rats (sham; Figure 1A). The tumor growth reached a peak at 16–19 days after tumor inoculation and regressed thereafter. Tumor size was insignificant 40 days after tumor cell inoculation. In PBS-injected control rats, the tumors grew continuously; rats were sacrificed 14 days after tumor inoculation. To evaluate leukocyte infiltration in the tumor tissues, some rats were sacrificed at 14 days after tumor cell inoculation, and tumor tissues were removed for immunohistochemistry analysis. The tumor weights measured on day 14 showed a significant difference between rat UCMSC- and PBSinjected groups (Figure 1B).

Rat UCMSC treatment stimulated infiltration of numerous lymphocytes into tumor

As shown in Figure 2A, PBS-treated orthotopic tumors in the mammary fat pad were composed of solidly packed round-to-oval cells. All tumor cells had irregularly shaped and irregularly sized nuclei with prominent nucleoli. Numerous mitotic figures were also commonly observed. Treatment with rat UCMSCs significantly increased the amount of extracellular matrix deposition and decreased the number of tumor cells within the tumor tissues (Figure 2B). In addition, treatment with rat UCMSCs caused infiltration of numerous lymphocytes but only a few neutrophils in the peri-tumoral area of the tumor mass. This leukocyte infiltration was not observed in the PBS control group (Figure 2A).

Rat UCMSC treatment increased infiltration of $CD4^+$ and $CD8^+$ T cells and NK cells and decreased macrophages and Treg cells in tumor

To identify TIL populations, immunohistochemistry analysis was performed using antibodies against CD3 (T cells), CD20 (B cells), CD4 (helper T cells), CD8 (cytotoxic T

cells), Foxp3 (Treg cells) and CD68 (monocytes/macrophages). As shown in Figure 3, treatment with rat UCMSCs caused a 3-fold increase of $CD3^+$ cells (average 150 cells/field) over the PBStreated control (average 50 cells/field). Treatment with rat UCMSCs also caused a 3-fold increase of $CD20^+$ cells (average 30 cells/field) over the control tumors. However, $CD20^+$ cells constituted only 20% of total lymphocytes infiltrating the tumor tissue after the treatment, indicating that the main component of lymphocytes in the tumor tissue was T cells rather than B cells (Figure 3). In the sub-population of T cells, treatment with rat UCMSCs significantly increased the number of both $CD4^+$ (3-fold) and $CD8^+$ (2-fold) cells (Figure 3). On average, $CD8^+$ cells were more numerous than $CD4^+$ cells. On the contrary, only a few $Foxp3^+$ cells were observed in the PBS group but not in the rat UCMSC-treated group (Figure 3). Although NK cells were not a major component of the TILs, NK cells were also significantly higher (1.8-fold higher) in the rat UCMSC-treated group than in the control group. $CD68^+$ cells were infrequently observed in the PBS group but not in the tumors treated with rat UCMSCs (Figure 3). These results indicate that treatment with rat UCMSCs caused the tumor tissue infiltration of helper and cytotoxic T cells and NK cells but decreased Treg cells and monocytes/macrophages.

Microarray analysis of cytokines related to cell migration

Gene expression of rat UCMSCs co-cultured with Mat B III was compared with naïve rat UCMSCs. A partial list of the highly up-regulated or down-regulated chemokines, cytokines and immune cell migration-related genes that showed >1.5 times difference in Z ratio is presented in Table I. Expression of MCP-1 was significantly increased in rat UCMSCs (13.88-fold) when they were co-cultured with Mat B III cells. Because MCP-1 is a chemoattractant associated with lymphocyte infiltration, MCP-1 is a potential candidate for stimulating lymphocyte migration in rat UCMSC-treated tumors.

MCP-1 expression was increased in rat UCMSCs when they were co-cultured with Mat B III cells

To confirm the aforementioned messenger RNA expression results from microarray analysis in protein levels, the expression of MCP-1 was semi-quantified by Western blot analysis. As shown in Figure 4, the basal expression of MCP-1 in rat UCMSCs was significantly larger than that in Mat B III. The expression of MCP-1 in rat UCMSCs was significantly increased when they were co-cultured with Mat B III cells. These results suggest that MCP-1 expression is sensitively up-regulated in response to the presence of Mat B III mammary carcinoma cells.

Rat UCMSCs stimulated PBMC migration by MCP-1 secretion

To examine whether PBMCs migrate toward rat UCMSCs and whether this migration is controlled by MCP-1, PBMC migration was examined by the Boyden chamber assay using the Transwell culture system in the presence or absence of MCP-1 neutralizing antibody. As shown in Figure 5, rat UCMSCs increased approximately 2-fold the infiltration of PBMCs into the Matrigel-coated membrane of the Transwell insert. The number of migrating PBMCs was significantly decreased by adding 4 mg/well of neutralizing antibody against MCP-1, indicating that the secretion of MCP-1 from rat UCMSCs is an important factor for migration of PBMCs, which are mainly lymphocytes. In the control study, the treatment of Mat B III with neutralizing antibody against MCP-1 did not show much effect on the infiltration of PBMCs to the bottom of the Transwell membrane. This result suggests that PBMC migration toward rat UCMSCs is specific. In the control experiment with anti-green fluorescent protein antibody instead of MCP-1 antibody, the number of the membrane-infiltrating PBMCs was slightly higher than without any antibody, but no statistically significant difference was observed. These results suggest that the effect of the MCP-1

antibody is specific, and PBMCs specifically migrate toward rat UCMSCs by sensing the MCP-1 gradient.

Discussion

It has been shown that stem cells are useful therapeutic tools for various diseases including cancers. UCMSCs are unique mesenchymal stem cells (2,3) and are considered to be safe therapeutic cells because systemic or subcutaneous administration of UCMSCs does not result in adverse effects or tumor formation in the recipients (4,31). In preclinical animal studies involving the use of naïve UCMSCs for cancer treatment, rat UCMSCs have demonstrated a remarkable ability to cause complete regression of Mat B III rat mammary tumors *in vivo* (1). In addition, un-engineered human UCMSCs were shown to attenuate human breast cancer xenografts in a SCID mouse model (5). However, the mechanism by which naïve UCMSCs attenuate tumor growth has yet to be fully understood. Although previous studies have demonstrated that diffusible factors produced by naïve UCMSCs play important roles in attenuation of the growth of tumor cells *in vitro*, the nature of factors and the mechanisms of *in vivo* tumor growth attenuation are yet to be clarified. The present study was focused on clarifying the mechanism by which rat UCMSCs attenuate the growth of mammary tumors both *in vitro* and in an *in vivo* rat model. The present study shows that rat UCMSCs enhance host anti-tumor immune responses by recruiting primarily $CD4^+$ and $CD8^+$ T cells and NK cells to tumor tissues, significantly attenuating mammary tumor growth. The results further suggest that a potential mechanism by which naïve rat UCMSCs increase lymphocyte infiltration into the tumor tissues is due to the increase of MCP-1 secretion.

The present study showed that treatment with naïve rat UCMSCs significantly attenuated the growth of orthotopic rat mammary tumors (Figure 1). This finding is consistent with the previous reports (1), in which a single treatment with rat UCMSCs completely abolished rat mammary tumors. Immunohistochemistry analysis of tumor tissues treated with rat UCMSCs revealed a significant increase of lymphocyte infiltration in the tumor tissues (Figure 2). Detailed analysis further revealed that the major component of infiltrating lymphocytes in rat UCMSC-treated tumor tissues is $CD8^+$ cells (approximately 52% of total lymphocytes are $CD8^+$ T cells and 37.5% cells correspond to $CD4^+$ T cells) (Figure 3). Although $CD20^+$ cells were also increased in the rat UCMSC-treated tumors, $CD20^+$ cells constituted <12% of total lymphocytes (Figure 3). In addition, a unique discovery in the present study was that no $CD68^+$ or $Foxp3^+$ cells were detected in tumor tissues in rat UCMSC-treated mice (Figure 3E), although a few $CD68^+$ and $Foxp3^+$ cells were consistently detected in untreated tumors. These results strongly suggest that treatment with naïve rat UCMSCs significantly enhanced host tumor immune responses by increasing $CD8^+$ cytotoxic T cells and decreasing $CD68^+$ macrophages and $Foxp3^+$ Treg cells. In various human cancers, it has been shown that TILs, such as cytotoxic T cells ($CD8^+$), helper T cells ($CD4^+$) and Treg cells ($Foxp3^+$), play important roles in controlling tumor growth (26). Among those TILs, $CD8^+$ T cells are the major subset of T cells, and they can become tumor-specific cytotoxic cells by direct recognition of tumor antigens presented on the tumor cells (24). Infiltration of $CD8^+$ T cells in the tumor site is shown to be associated with a good prognosis in malignant tumors such as colorectal, ovarian and esophageal carcinoma (20–23). These reports support the idea that rat UCMSC-dependent tumor growth attenuation is associated with stimulation of host anti-tumor immune responses via $CD8^+$ T cell infiltration in the tumor tissues. An increase of $CD4^+$ helper T cells in rat UCMSC-treated tumors (Figure 3) further supports the idea of stimulation of host anti-tumor immune responses because helper T cells assist in activation and proliferation of cytotoxic T cells (32). Decrease of Treg cells also supports an increase of cytotoxic T cells because they directly attenuate T-cell proliferation (33). Therapies to decrease the Treg cell population or

to blunt the function of Treg cells are effective in attenuating various tumors (34). In contrast, numerous reports indicate that an increase of Treg cells in tumor tissues correlates with tumor progression and poor prognosis of multiple organ type cancers including breast cancer (35).

In the present study, treatment with rat UCMSCs also increased NK cells in tumor tissues (Figure 3). Because NK cells are an important component of anti-tumor immune reactions in addition to cytotoxic T cells, an increase of NK cells enhances antitumor immune reactions. Although NK cells are innate immune cells and do not have the specificity to particular tumors, they quickly induce apoptosis in tumor cells attenuating tumor burden (36). Taken together, these results clearly indicate that treatment with rat UCMSCs increases the infiltration of $CD8^+$ T cells and NK cells into tumor tissues and decreases $CD68^+$ macrophages and $Foxp3^+$ Treg cells, reducing the tumor volume. The granzyme-positive population in the $CD8^+$ T cells in the tumor tissues should be clarified in future studies.

Our results from the present study indicate that rat PBMC migration is directed toward rat UCMSCs rather than Mat B III mammary carcinoma cells (Figure 5). This migration is associated with MCP-1 because MCP-1 neutralizing antibody attenuates PBMC migration to the rat UCMSCs (Figure 5). This finding is directly relevant to the histologic findings showing that intratumoral injection of rat UCMSCs induced infiltration of numerous lymphocytes into the tumor tissues (Figure 2 and Figure 3). MCP-1 is shown to play an important role in migration of lymphocytes and NK cells to tumor tissues. MCP-1 is a member of the chemokine-2 subfamily that attracts and activates monocytes or lymphocytes at sub-nanomolar concentrations (37–39). Expression of MCP-1 in tumor tissues is shown to be sufficient for induction of cytotoxic T-cell migration to tumor tissues in mouse xenograft studies (40). Tsuchiyama *et al.* (41) reported that a therapy with recombinant adenovirus vector expressing suicide gene, HSV thymidine kinase, and MCP-1 completely eradicated hepatocellular carcinoma by the recruitment of NK cells. The present study suggests that rat UCMSCs traffic to tumor tissues and recruit T cells to the tumor site through increased MCP-1 secretion. To the best of our knowledge, this study is the first report showing that rat UCMSCs secrete a chemoattractant such as MCP-1 and induce lymphocyte infiltration. This report suggests that MCP-1 could be a potential therapeutic target to enhance local immune responses to attenuate mammary carcinoma.

$CD68^+$ cells were not observed in the rat UCMSC-treated tumors despite the fact that $CD68^+$ macrophages are known to be attracted by MCP-1 (42). The likely explanation is that a factor inhibitory to macrophages might be secreted from rat UCMSCs or Mat B III cells. The microarray analysis indicated that the expression of macrophage inhibitory factor (MIF) was significantly increased (3.4-fold) in rat UCMSCs co-cultured with Mat B III cells (Table I). It is likely that increased MIF expression may have stimulated an exodus of macrophages from the rat UCMSC-treated tumors, assisting rat UCMSC-dependent attenuation of tumor growth. Clarification of the role of MIF in rat UCMSC-treated tumors requires further studies.

Regarding macrophage infiltration in the tumor tissues, clinical studies have sought to identify correlations between macrophage density and prognosis. A summary in a review by Bingle *et al.* (43) using a meta-analysis showed that in >80% of the cases, an increased macrophage density in tumor tissues was associated with poor prognosis, and the remaining 20% of cases were split between cases having no effect and cases with good prognosis. This association was confirmed with simple histologic evaluation of macrophage density, which showed that macrophage density in itself was an independent predictor of poor outcome (44,45). In consideration of these reports, the micro-environment without macrophages results in a better probability for attenuating tumor growth. However, further experiments

are required to clarify the relationship between the decrease of macrophage density and the effect of rat UCMSCs on tumor growth attenuation.

Among many tissue-originated multipotent stem cells, UCMSCs are very usable owing to unethical abundant resources, the simplicity of their preparation method (46), bankability (47), low immunogenicity (48,49) and tropism to inflammatory tissues such as tumor tissues (1,4,6). In particular, human UCMSCs apparently escape the host immune responses by multiple mechanisms (8); they express major histocompatibility complex class I but not class II antigens; they are negative for other costimulatory antigens such as CD80 and CD86 (50,51); they produce large amounts of tolerogenic interleukin-10 and transforming growth factor-β and express human leukocyte antigen G (HLA-G) at higher levels than bone marrow-derived mesenchymal stem cells (50–52). This poor immunogenicity allows human UCMSCs to be usable for allogeneic transplantation in potential human applications. In relation to this poor immunogenicity, Chao *et al.* (53) reported a successful transplantation of human UCMSC-derived islet-like cells in diabetic rats without using immunosuppressants. The tropism of UCMSCs to the inflammatory tissues, such as tumor tissues, makes this cell usable as targeted drug or gene delivery vehicles. More recent reports have shown that human UCMSCs engineered to express interferon-β, which is a strong apoptosis inducer, migrated to metastatic human breast tumor nodules in the lung (4) or to the bronchioloalveolar carcinoma nodules (6), produced sufficient amounts of the interferon-β in the tumor tissues and significantly attenuated tumor growth in mice. Human UCMSCs engineered to express MCP-1 are expected to migrate to the tumor tissues, recruit large numbers of $CD8^+$ T cells, $CD4^+$ T cells and NK cells to the tumor sites and control tumor growth. To ensure these potential applications, further studies are needed to confirm the abovementioned possibilities. Although a live cell therapy with multipotent stem cells holds significant possibilities, a potential limitation of this cell therapy could be a migration to unexpected tissues and differentiations. The safety of live cell therapy and the fate of multipotent stem cells in the human body should be carefully clarified in the future.

In conclusion, bolus treatment with naïve rat UCMSCs significantly attenuated the growth of orthotopic rat mammary carcinoma grafts. This tumor growth attenuation is associated with a marked increase of $CD8^+$ and $CD4^+$ T-cell and NK cell infiltration and escape of $CD68^+$ macrophages and $Foxp3^+$ Treg cells from tumor tissues. Recruitment of T cells and NK cells and an escape of $CD68^+$ cells appear to be mediated by MCP-1 and MIF, and they were secreted mainly from rat UCMSCs. Rat UCMSCs traffic to tumor tissues and recruit cytotoxic lymphocytes by the secretion of lymphocyte migration cytokines such as MCP-1 and MIF, controlling tumor growth. UCMSC-based cytotherapy may be a new therapeutic modality for the treatment of mammary carcinoma.

Acknowledgments

We are grateful to Mr William H. Wood III (National Institute on Aging, NIH) for his excellent technical assistance in microarray analysis. We are thankful to Mr Sivasai Balivada (Department of Anatomy & Physiology, Kansas State University) for his technical assistance in animal studies. This work was supported by Kansas State University (KSU) Terry C. Johnson Center for Basic Cancer Research, Kansas Bioscience Authority Collaborative Cancer Research Initiative grant, Kansas State Legislative Appropriation, KSU College of Veterinary Medicine Dean's fund, NIH grants P20 RR017686, P20 RR016475, P20 RR01556 and R21 CA135599 and the Intramural Research Program of the NIH, National Institute on Aging.

References

1. Ganta C, Chiyo D, Ayuzawa R, Rachakatla R, Pyle M, Andrews G, et al. Rat umbilical cord stem cells completely abolish rat mammary carcinomas with no evidence of metastasis or recurrence 100 days post-tumor cell inoculation. Cancer Res. 2009; 69:1815–1820. [PubMed: 19244122]

2. Weiss ML, Medicetty S, Bledsoe AR, Rachakatla RS, Choi M, Merchav S, et al. Human umbilical cord matrix stem cells: preliminary characterization and effect of transplantation in a rodent model of Parkinson's disease. Stem Cells. 2006; 24:781–792. [PubMed: 16223852]
3. Troyer DL, Weiss ML. Wharton's jelly-derived cells are a primitive stromal cell population. Stem Cells. 2008; 26:591–599. [PubMed: 18065397]
4. Rachakatla RS, Marini F, Weiss ML, Tamura M, Troyer D. Development of human umbilical cord matrix stem cell-based gene therapy for experimental lung tumors. Cancer Gene Ther. 2007; 14:828–835. [PubMed: 17599089]
5. Ayuzawa A, Doi C, Rachakatla RS, Pyle MM, Maurya DK, Troyer D, et al. Naïve human umbilical cord matrix derived stem cells significantly attenuate growth of human breast cancer cells in vitro and in vivo. Cancer Lett. 2009; 280:31–37. [PubMed: 19285791]
6. Matsuzuka T, Rachakatla RS, Doi C, Maurya DK, Ohta N, Kawabata A, et al. Human umbilical cord matrix-derived stem cells expressing interferon-beta gene significantly attenuate bronchioloalveolar carcinoma xenografts in SCID mice. Lung Cancer. 2010; 70:28–36. [PubMed: 20138387]
7. Chao KC, Yang HT, Chen MW. Human umbilical cord mesenchymal stem cells suppress breast cancer tumorigenesis through direct cell-cell contact and internalization. J Cell Mol Med. 2012; 16:1803–1815. [PubMed: 21973190]
8. Tamura M, Kawabata A, Ohta N, Uppalapati L, Becker K, Troyer D. Wharton's jelly stem cells as agents for cancer therapy. Open Tissue Eng Regen Med J. 2011; 4:39–47.
9. van Roozendaal KE, Klijn JG, van Ooijen B, Claassen C, Eggermont AM, Henzen-Logmans SC, et al. Differential regulation of breast tumor cell proliferation by stromal fibroblasts of various breast tissue sources. Int J Cancer. 1996; 65:120–125. [PubMed: 8543388]
10. Barcellos-Hoff MH, Ravani SA. Irradiated mammary gland stroma promotes the expression of tumorigenic potential by unirradiated epithelial cells. Cancer Res. 2000; 60:1254–1260. [PubMed: 10728684]
11. Shekhar MP, Werdell J, Santner SJ, Pauley RJ, Tait L. Breast stroma plays a dominant regulatory role in breast epithelial growth and differentiation: implications for tumor development and progression. Cancer Res. 2001; 61:1320–1326. [PubMed: 11245428]
12. Sadlonova A, Novak Z, Johnson MR, Bowe DB, Gault SR, Page GP, et al. Breast fibroblasts modulate epithelial cell proliferation in three-dimensional in vitro co-culture. Breast Cancer Res. 2005; 7:R46–R59. [PubMed: 15642169]
13. Fleming JM, Miller TC, Quinones M, Xiao Z, Xu X, Meyer MJ, et al. The normal breast microenvironment of premenopausal women differentially influences the behavior of breast cancer cells in vitro and in vivo. BMC Med. 2010; 8:27. [PubMed: 20492690]
14. Karlan BY, Baldwin RL, Cirisano FD, Mamula PW, Jones J, Lagasse LD. Secreted ovarian stromal substance inhibits ovarian epithelial cell proliferation. Gynecol Oncol. 1995; 59:67–74. [PubMed: 7557618]
15. Dong-Le, Bourhis X.; Berthois, Y.; Millot, G.; Degeorges, A.; Sylvi, M.; Martin, PM., et al. Effect of stromal and epithelial cells derived from normal and tumorous breast tissue on the proliferation of human breast cancer cell lines in co-culture. Int J Cancer. 1997; 71:2–8.
16. Arnold JT, Lessey BA, Seppälä M, Kaufman DG. Effect of normal endometrial stroma on growth and differentiation in Ishikawa endometrial adenocarcinoma cells. Cancer Res. 2002; 62:79–88. [PubMed: 11782363]
17. Proia DA, Kuperwasser C. Stroma: tumor agonist or antagonist. Cell Cycle. 2005; 8:1022–1025. [PubMed: 16082203]
18. Disis ML, Bernhard H, Jaffee EM. Use of tumour-responsive T cells as cancer treatment. Lancet. 2009; 373:673–683. [PubMed: 19231634]
19. Kasper HU, Drebber U, Stippel DL, Dienes HP, Gillessen A. Liver tumor infiltrating lymphocytes: comparison of hepatocellular and cholangiolar carcinoma. World J Gastroenterol. 2009; 15:5053–5057. [PubMed: 19859998]
20. Schumacher K, Haensch W, Röefzaad C, Schlag PM. Prognostic significance of activated CD8(+) T cell infiltrations within esophageal carcinomas. Cancer Res. 2001; 61:3932–3936. [PubMed: 11358808]

21. Zhang L, Conejo-Garcia JR, Katsaros D, Gimotty PA, Massobrio M, Regnani G, et al. Intratumoral T cells, recurrence, and survival in epithelial ovarian cancer. N Engl J Med. 2003; 348:203–213. [PubMed: 12529460]
22. Menon AG, Jansen-van Rhijin C, Morreau H, Putter H, Tollenaar RA, van de Velde CJ, et al. Immune system and prognosis in colorectal cancer: a detailed immunohistochemical analysis. Lab Invest. 2004; 84:493–501. [PubMed: 14968119]
23. Prall F, Dührkop T, Weirich V, Ostwald C, Lenz P, Nizze H, et al. Prognostic role of CD8+ tumor-infiltrating lymphocytes in stage III colorectal cancer with and without microsatellite instability. Hum Pathol. 2004; 35:808–816. [PubMed: 15257543]
24. Ryschich E, Cebotari O, Fabian OV, Autschbach F, Kleeff J, Friess H, et al. Loss of heterozygosity in the HLA class I region in human pancreatic cancer. Tissue Antigens. 2004; 64:696–702. [PubMed: 15546343]
25. Jonuleit H, Schmitt E, Stassen M, Tuettenberg A, Knop J, Enk AH. Identification and functional characterization of human CD4(+)CD25(+) T cells with regulatory properties isolated from peripheral blood. J Exp Med. 2001; 193:1285–1294. [PubMed: 11390435]
26. Curtin JF, Candolfi M, Fakhouri TM, Liu C, Alden A, Edwards M, et al. Treg depletion inhibits efficacy of cancer immunotherapy: implications for clinical trials. PLoS One. 2008; 3:e1983. [PubMed: 18431473]
27. Pockaj BA, Sherry RM, Wei JP, Yannelli JR, Carter CS, Leitman SF, et al. Localization of 111indium-labeled tumor infiltrating lymphocytes to tumor in patients receiving adoptive immunotherapy: augmentation with cyclophosphamide and correlation with response. Cancer. 1994; 73:1731–1737. [PubMed: 8156501]
28. Li J, Chigurupati S, Agarwal R, Mughal MR, Mattson MP, Becker KG, et al. Possible angiogenic roles for claudin-4 in ovarian cancer. Cancer Biol Ther. 2009; 8:1806–1814. [PubMed: 19657234]
29. Cheadle C, Vawter MP, Freed WJ, Becker KG. Analysis of microarray data using Z score transformation. J Mol Diagn. 2003; 5:73–81. [PubMed: 12707371]
30. Tsai WH, Shih CH, Lin CC, Ho CK, Hsu FC, Hsu HC. Monocyte chemotactic protein-1 in the migration of differentiated leukaemic cells toward alveolar epithelial cells. Eur Respir J. 2008; 31:957–962. [PubMed: 18216048]
31. Rachakatla RS, Pyle MM, Ayuzawa R, Edwards SM, Marini FC, Weiss ML, et al. Combination treatment of human umbilical cord matrix stem cell-based interferon-beta gene therapy and 5-fluorouracil significantly reduces growth of metastatic human breast cancer in SCID mouse lungs. Cancer Invest. 2008; 26:662–670. [PubMed: 18608205]
32. Abbas AK, Murphy KM, Sher A. Functional diversity of helper T lymphocytes. Nature. 1996; 383:787–793. [PubMed: 8893001]
33. Woo EY, Yeh H, Chu CS, Schlienger K, Carroll RG, Riley JL, et al. Cutting edge: regulatory T cells from lung cancer patients directly inhibit autologous T cell proliferation. J Immunol. 2002; 168:4272–4276. [PubMed: 11970966]
34. Colombo MP, Piconese S. Regulatory-T-cell inhibition versus depletion: the right choice in cancer immunotherapy. Nat Rev Cancer. 2007; 7:880–887. [PubMed: 17957190]
35. Beyer M, Schultze JL. Regulatory T cells in cancer. Blood. 2006; 108:804–811. [PubMed: 16861339]
36. Zamai L, Ponti C, Mirandola P, Gobbi G, Papa S, Galeotti L, et al. NK cells and cancer. J Immunol. 2007; 178:4011–4016. [PubMed: 17371953]
37. Leonard EJ, Yoshimura T. Human monocyte chemoattractant protein-1 (MCP-1). Immunol Today. 1990; 11:97–101. [PubMed: 2186747]
38. Oppenheim JJ, Zachariae CO, Mukaida N, Matsushima K. Properties of the novel proinflammatory supergene “intercrine” cytokine family. Annu Rev Immunol. 1991; 9:617–648. [PubMed: 1910690]
39. Carr MW, Roth SJ, Luther E, Rose SS, Springer TA. Monocyte chemoattractant protein 1 acts as a T-lymphocyte chemoattractant. Proc Natl Acad Sci U S A. 1994; 91:3652–3656. [PubMed: 8170963]

40. Brown CE, Vishwanath RP, Aguilar B, Starr R, Najbauer J, Aboody KS, et al. Tumor-derived chemokine MCP-1/CCL2 is sufficient for mediating tumor tropism of adoptively transferred T cells. J Immunol. 2007; 179:3332–3341. [PubMed: 17709550]
41. Tsuchiyama T, Nakamoto Y, Sakai Y, Marukawa Y, Kitahara M, Mukaida N, et al. Prolonged, NK cell-mediated antitumor effects of suicide gene therapy combined with monocyte chemoattractant protein-1 against hepatocellular carcinoma. J Immunol. 2007; 178:574–583. [PubMed: 17182598]
42. Maus UA, Waelsch K, Kuziel WA, Delbeck T, Mack M, Blackwell TS, et al. Monocytes are potent facilitators of alveolar neutrophil emigration during lung inflammation: role of the CCL2-CCR2 axis. J Immunol. 2003; 170:3273–3278. [PubMed: 12626586]
43. Bingle L, Brown NJ, Lewis CE. The role of tumor-associated macrophages in tumor progression: implications for new anticancer therapies. J Pathol. 2002; 196:254–265. [PubMed: 11857487]
44. Dave SS, Wright G, Tan B, Rosenwald A, Gascoyne RD, Chan WC, et al. Prediction of survival in follicular lymphoma based on molecular features of tumor-infiltrating immune cells. N Engl J Med. 2004; 351:2159–2169. [PubMed: 15548776]
45. Farinha P, Masoudi H, Skinnider BF, Shumansky K, Spinelli JJ, Gill K, et al. Analysis of multiple biomarkers shows that lymphoma-associated macrophage (LAM) content is an independent predictor of survival in follicular lymphoma (FL). Blood. 2005; 106:2169–2174. [PubMed: 15933054]
46. Mitchell KE, Weiss ML, Mitchell BM, Martin P, Davis D, Morales L, et al. Matrix cells from Wharton's jelly form neurons and glia. Stem Cells. 2003; 21:50–60. [PubMed: 12529551]
47. Gong W, Han Z, Zhao H, Wang Y, Wang J, Zhong J, et al. Banking human umbilical cord-derived mesenchymal stromal cells for clinical use. Cell Transplant. 2012; 21:207–216. [PubMed: 21929848]
48. Cho PS, Messina DJ, Hirsh EL, Chi N, Goldman SN, Lo DP, et al. Immunogenicity of umbilical cord tissue derived cells. Blood. 2008; 111:430–438. [PubMed: 17909081]
49. Weiss ML, Anderson C, Medicetty S, Seshareddy KB, Weiss RJ, VanderWerff I, et al. Immune properties of human umbilical cord Wharton's jelly-derived cells. Stem Cells. 2008; 26:2865–2874. [PubMed: 18703664]
50. La, Rocca G.; Anzalone, R.; Corrao, S.; Magno, F.; Loria, T.; Lo, Iacono M., et al. Isolation and characterization of Oct-4+/ HLA-G+ mesenchymal stem cells from human umbilical cord matrix: differentiation potential and detection of new markers. Histochem Cell Biol. 2009; 131:267–282. [PubMed: 18836737]
51. Prasanna SJ, Gopalakrishnan D, Shankar SR, Vasandan AB. Pro-inflammatory cytokines, IFNgamma and TNFalpha, influence immune properties of human bone marrow and Wharton jelly mesenchymal stem cells differentially. PLoS One. 2010; 5:e9016. [PubMed: 20126406]
52. Deuse T, Stubbendorff M, Tang-Quan K, Phillips N, Kay MA, Eiermann T, et al. Immunogenicity and immunomodulatory properties of umbilical cord lining mesenchymal stem cells. Cell Transplant. 2011; 20:655–667. [PubMed: 21054940]
53. Chao KC, Chao KF, Fu YS, Liu SH. Islet-like clusters derived from mesenchymal stem cells in Wharton's jelly of the human umbilical cord for transplantation to control type 1 diabetes. PLoS One. 2008; 3:e1451. [PubMed: 18197261]

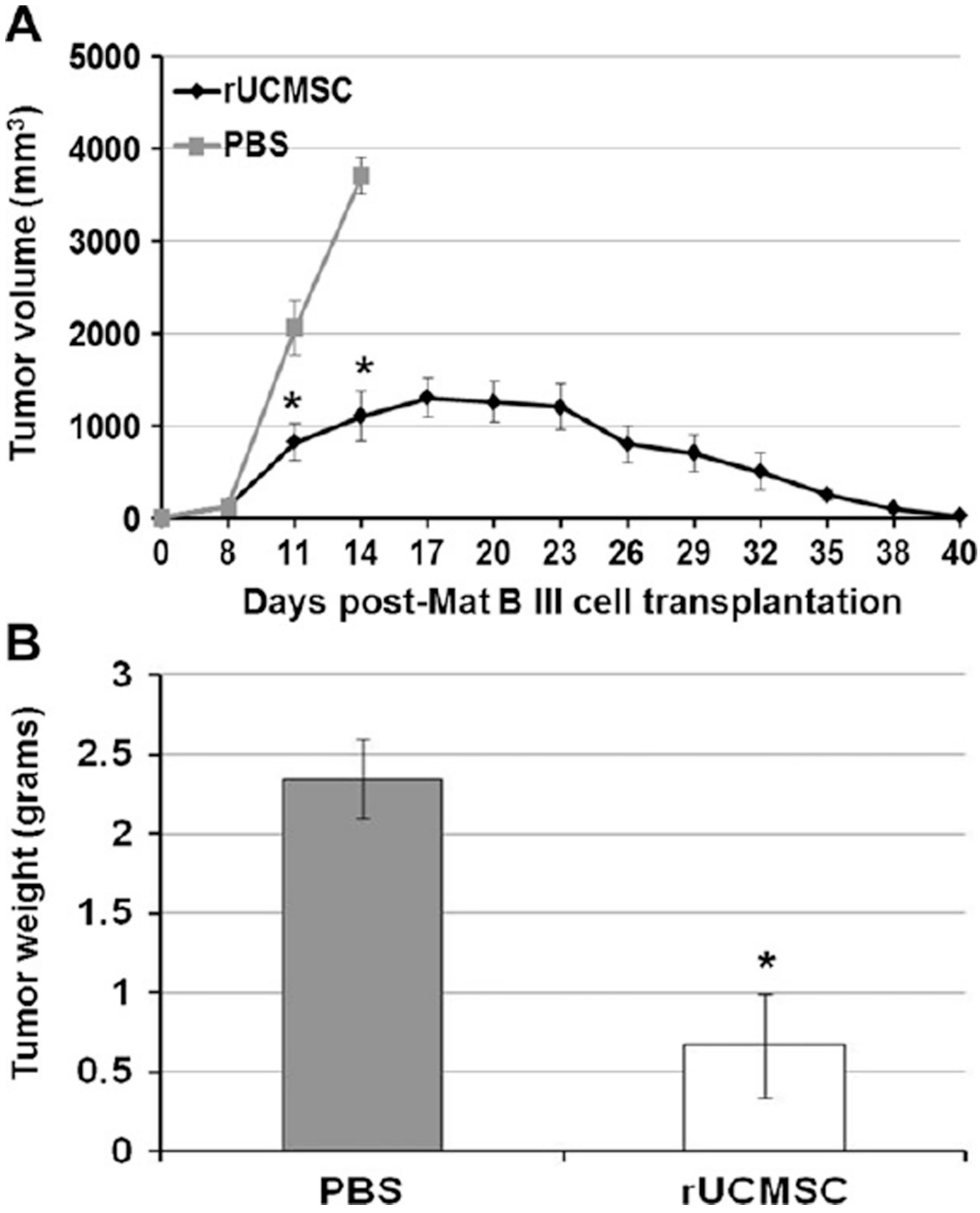

Figure 1.

Bolus injection of naïve rat UCMSCs in tumors completely attenuated the growth of orthotopic Mat B III grafts in a syngeneic F344 rat model. A single intratumoral injection of rat UCMSCs (1 million cells, n = 9) significantly attenuated the Mat B III tumor growth curve (1 million Mat B III cells) and completely regressed the tumors at day 40 (A). Five each of rat UCMSC-treated or PBS-treated rats were sacrificed 14 days after tumor cell inoculation. The average tumor weight in rat UCMSC-treated rats was significantly smaller than in PBS-treated rats (n = 5) (B). $*P < 0.05$ compared with PBS-treated control.

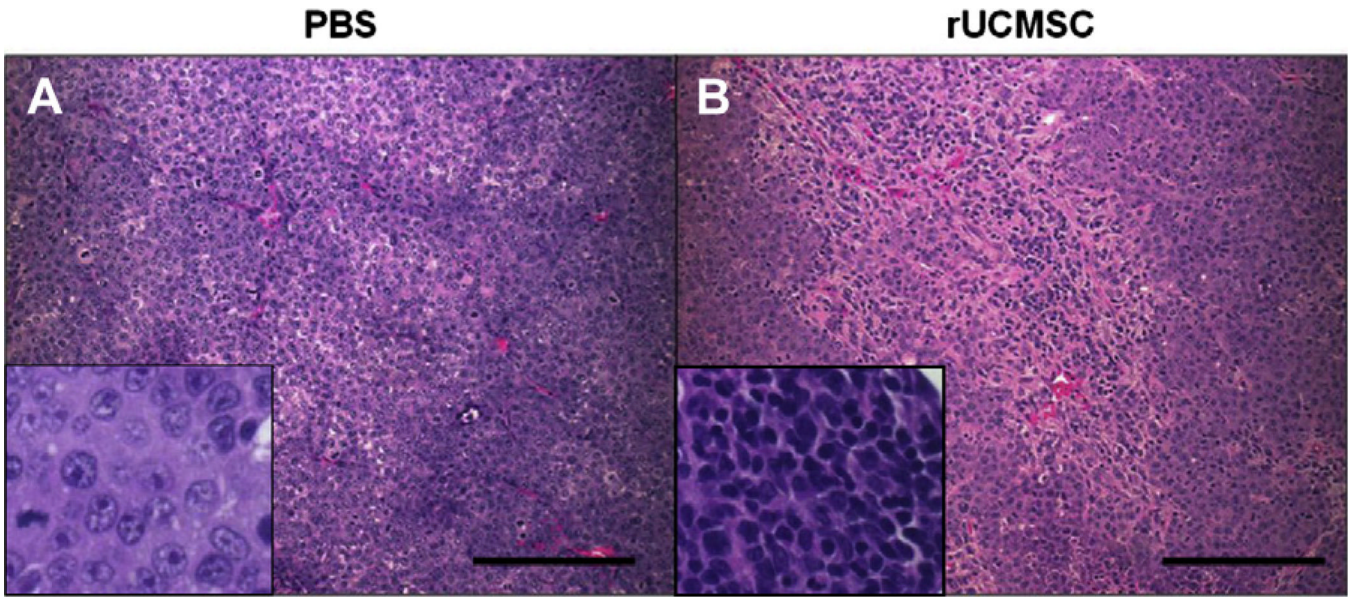

Figure 2.

Mononuclear leukocyte infiltration was significantly increased in rat UCMSC-treated orthotopic Mat B III grafts. Samples were prepared as described in Methods and subjected to histologic analysis after hematoxylin and eosin staining. Typical PBS-treated and rat UCMSC-treated tumors are shown. (A) Most cells in the PBS-treated tumors are tumor cells (inset). (B) A large portion of the tumor was composed of connective tissues (areas with pinkish color) and a large number of mononuclear cells (inset). (Scale bars = 200 μm.)

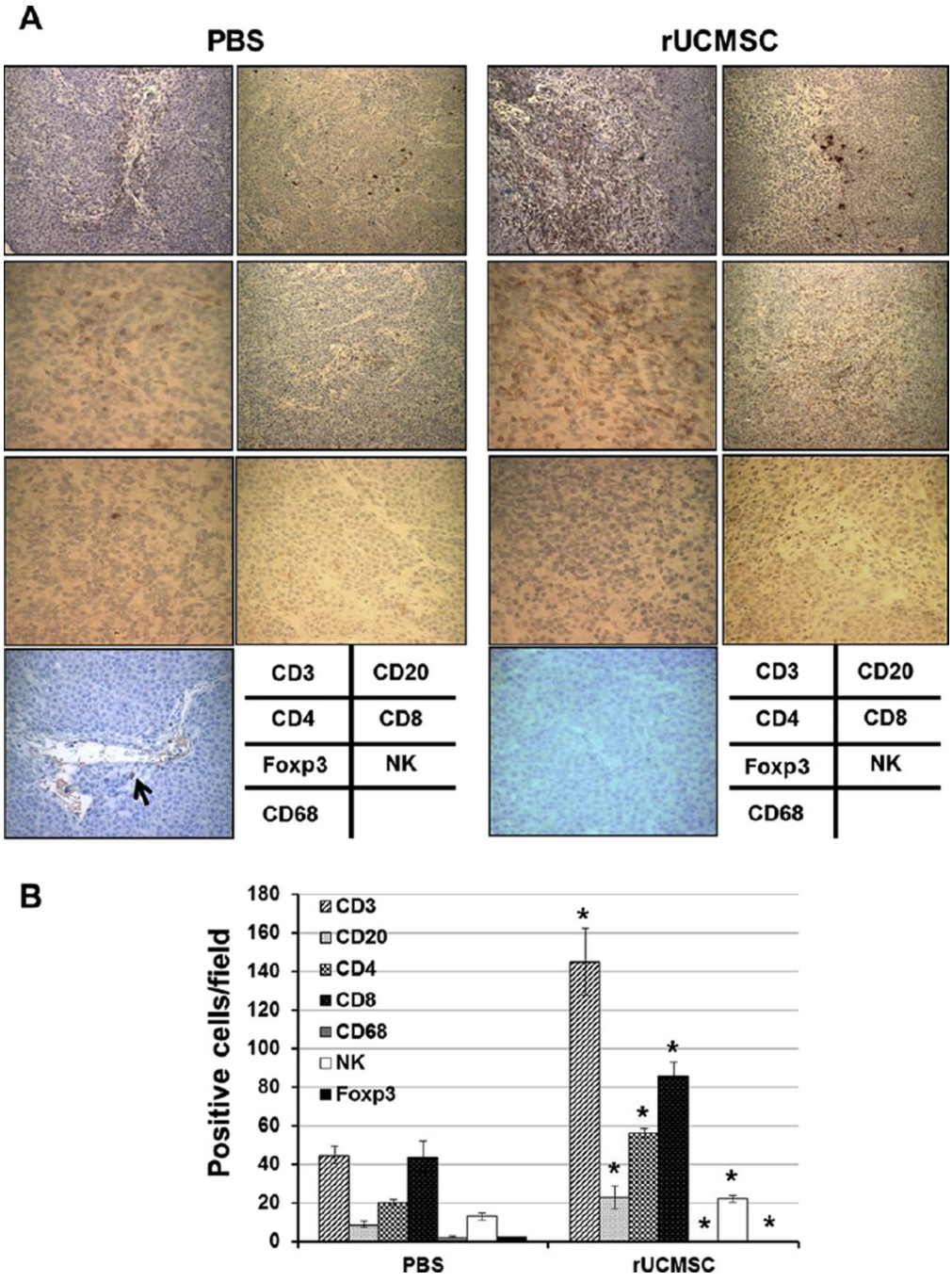

Figure 3.

Detection of specific lymphocyte populations in PBS-treated and rat UCMSC-treated tumors. Treatment with rat UCMSCs significantly stimulated infiltration of CD3, CD4, CD20, $CD8^+$ and NK cells but attenuated $Foxp3^+$ and $CD68^+$ cells in Mat B III mammary tumors. Samples were prepared and subjected to immunohistochemistry analysis as described in Methods. (A) Typical pictures of each antibody staining are shown. The original magnification of pictures of CD3, CD20, CD8, NK marker and CD68 is 100× and of CD4 and Foxp3 is 200×. (B) The average number of each cell type (bar graphs) was determined by analyzing 10 tumor areas in each treatment group and expressed as cell

number per high-power field (400×). The arrow in (A) shows a $CD68^+$ cell. $*P < 0.05$ compared with PBS-treated control.

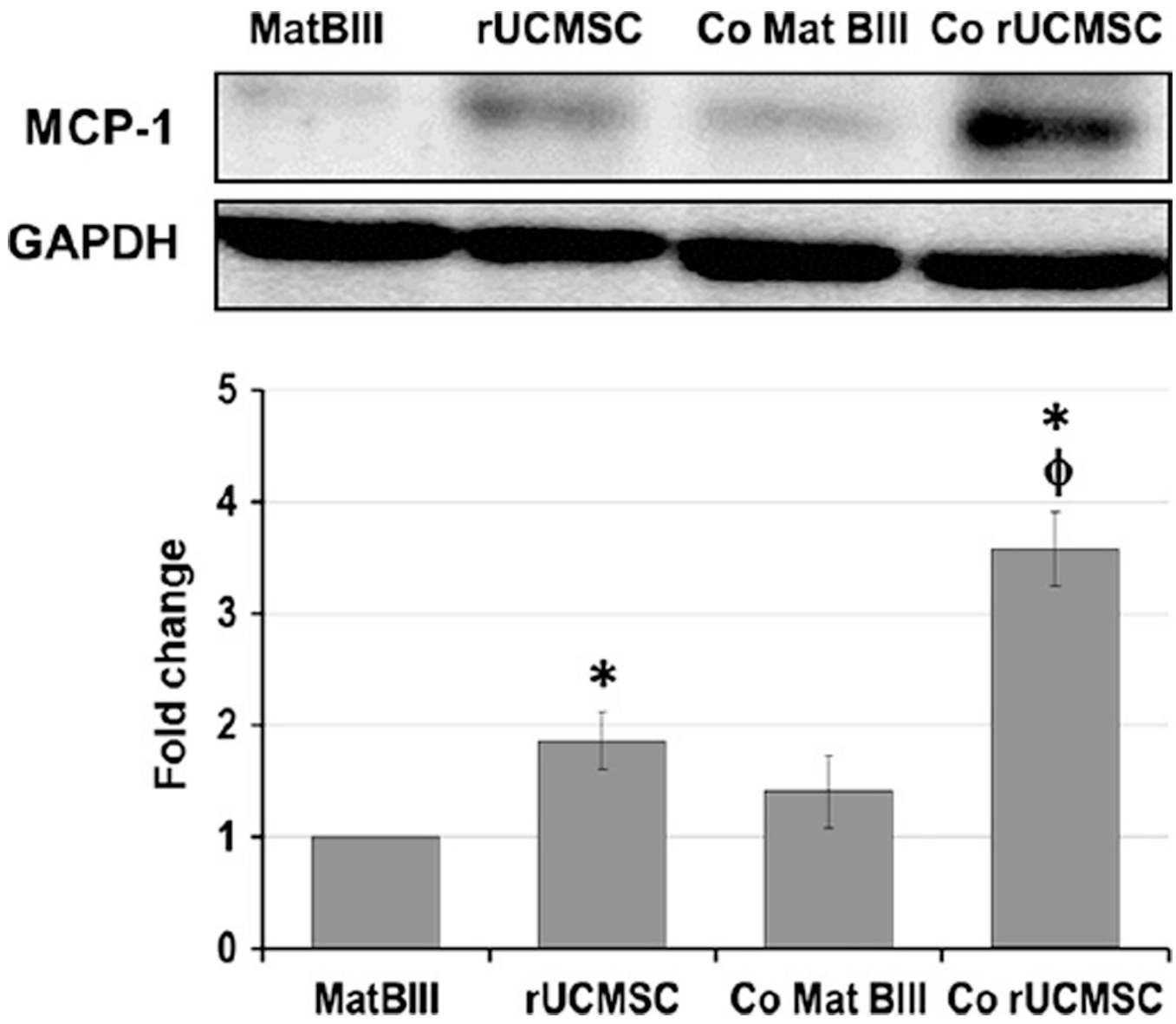

Figure 4.

Indirect co-culture of a small number of rat UCMSCs and Mat B III cells significantly increased MCP-1 expression in rat UCMSCs. The whole cell lysate from each cell type was separately prepared 3 days after co-culture and subjected to Western blot analysis. Samples were prepared as described in Methods. The average expression levels of MCP-1 were normalized by GAPDH and are displayed in the histogram. Sample preparation and Western blot analysis were performed three times with duplicate determinations. Typical blotting results are shown. *$P < 0.05$ compared with Mat B III. φ$P < 0.05$ compared with rat UCMSCs without co-culture.

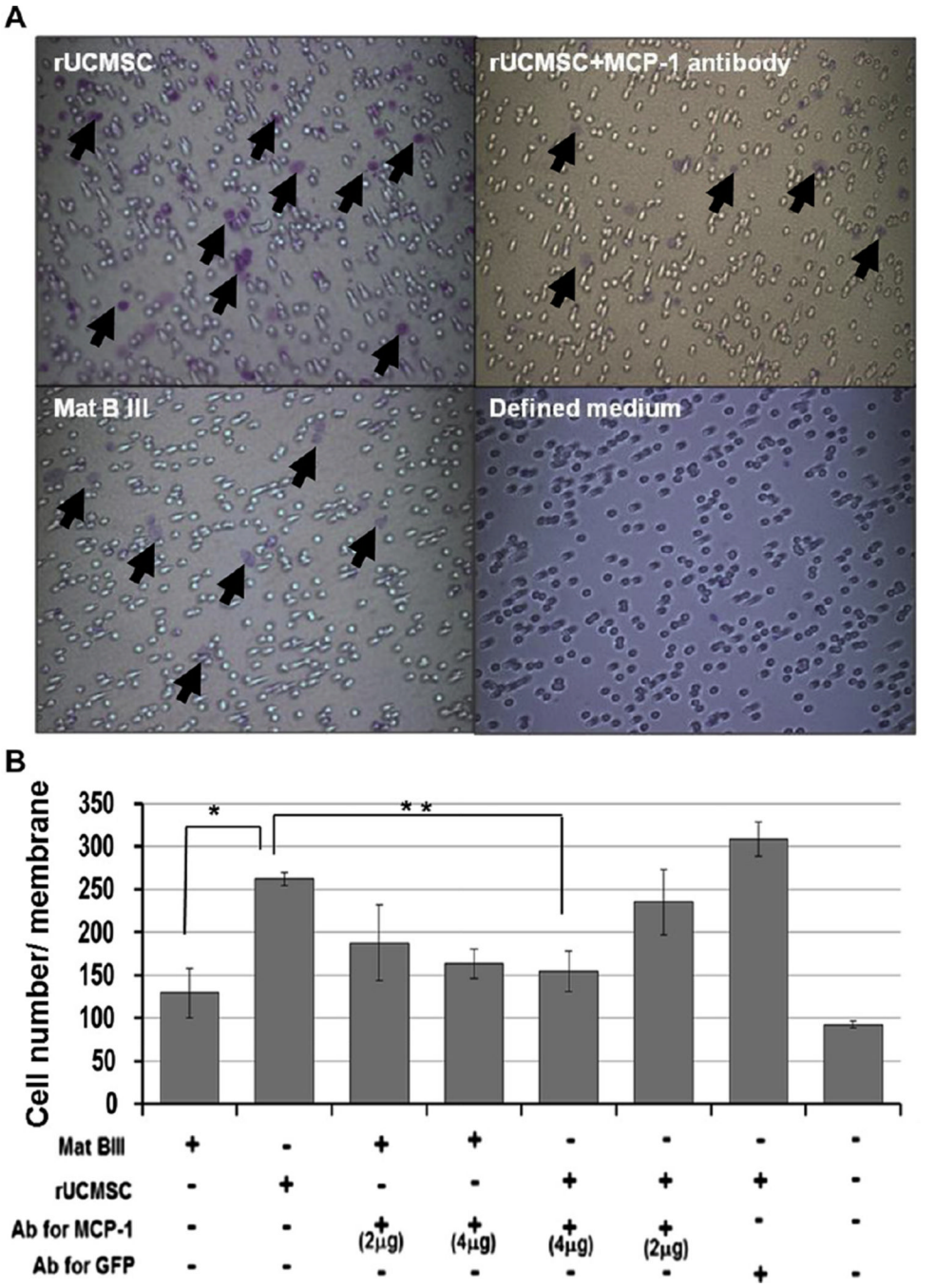

Figure 5.

Addition of anti-mouse MCP-1 antibodies significantly attenuated the migration of rat PBMCs toward either rat UCMSCs or Mat B III cells in the Boyden chamber assay. (A) Migrated PBMCs (purple-colored cells) are shown on the lower surface of the membrane. Antibody against MCP-1 was added in the lower chambers as noted. (B) Summarized results from migration assay. The experiment was performed twice with triplicate determinations. Arrows in (A) show the migrated leukocytes. *$P < 0.05$ compared with Mat B III cells. **$P < 0.05$ compared with rat UCMSCs.

Table I

Microarray analysis of naïve rat umbilical cord matrix stem cells and cells co-cultured with Mat B III mammary tumor cells.

Gene	Gene description	Z ratio of co-cultured rat UCMSC/naïve rat UCMSC
Ccl1	Chemokine (C-X-C motif) ligand 1 (melanoma growth stimulating activity, alpha)	16.05
Ccl2	Chemokine (C-C motif) ligand 2 (monocyte chemoattractant protein-1)	13.88
Ccl7	Chemokine (C-C motif) ligand 7	11.88
Il1rl1	Interleukin 1 receptor-like 1	7.82
Cxcl16	Chemokine (C-X-C motif) ligand 16	5.55
Fst	Follistatin	4.79
Ptrn	Protein tyrosine phosphatase receptor type N	4.10
Cxcl12	Chemokine(C-X-C motif) ligand 12 (stromal cell-derived factor 1)	3.70
Mif	Macrophage migration inhibitory factor	3.37
Ltbp2	Latent transforming growth factor beta binding protein 2	3.28
Csf1	Colony stimulating factor 1 (macrophage)	3.14
Maf	Monocyte to macrophage differentiation-associated	2.93
Tnfaip8_predicted	Tumor necrosis factor alpha-induced protein 8	2.47
Ifitm3	Interferon induced transmembrane protein 3	2.16
Htra1	HtrA serine peptide 1	1.91
Tnfrsf12a	Tumor necrosis factor receptor superfamily member 12a	1.16